



PUBLISHED BY INSTITUTE OF PHYSICS PUBLISHING FOR SISSA

RECEIVED: December 4, 2007

REVISED: February 11, 2008

ACCEPTED: February 25, 2008

PUBLISHED: March 10, 2008

On the impact of systematical uncertainties for the CP violation measurement in superbeam experiments

Patrick Huber

*Physics Department, Theory Division, CERN,
CH-1211 Geneva 23, Switzerland, and
Institute for Particle, Nuclear and Astronomical Sciences,
Physics Department, Virginia Tech,
Blacksburg, VA 24062, U.S.A.
E-mail: pahuber@vt.edu*

Mauro Mezzetto

*Istituto Nazionale Fisica Nucleare, Sezione di Padova,
Via Marzolo 8, 35100 Padova, Italy
E-mail: mauro.mezzetto@pd.infn.it*

Thomas Schwetz

*Physics Department, Theory Division, CERN,
CH-1211 Geneva 23, Switzerland
E-mail: schwetz@cern.ch*

ABSTRACT: Superbeam experiments can, in principle, achieve impressive sensitivities for CP violation in neutrino oscillations for large θ_{13} . We study how those sensitivities depend on assumptions about systematical uncertainties. We focus on the second phase of T2K, the so-called T2HK experiment, and we explicitly include a near detector in the analysis. Our main result is that even an idealised near detector cannot remove the dependence on systematical uncertainties completely. Thus additional information is required. We identify certain combinations of uncertainties, which are the key to improve the sensitivity to CP violation, for example the ratio of electron to muon neutrino cross sections and efficiencies. For uncertainties on this ratio larger than 2%, T2HK is systematics dominated. We briefly discuss how our results apply to a possible two far detector configuration, called T2KK. We do not find a significant advantage with respect to the reduction of systematical errors for the measurement of CP violation for this setup.

KEYWORDS: Neutrino Physics, Standard Model.

Contents

1. Introduction	1
2. Qualitative discussion	3
3. Neutrino cross sections	5
4. Description of the simulation	8
5. Results	10
5.1 CP violation at T2HK	10
5.2 Constraints on neutrino fluxes and properties of the near detector	13
5.3 Determination of θ_{13} at T2K and T2HK	16
5.4 T2KK	18
6. Summary and discussion	19
A. Experiment simulation and systematics treatment	21
A.1 Detector simulation	21
A.2 χ^2 definition and systematics	22
B. A far detector-only setup with effective systematics	24

1. Introduction

Neutrino oscillation offers a natural, minimalistic framework to account for the observed data in a wide variety of experiments. It has been established as the leading mechanism for flavour transitions in solar [1, 2] and atmospheric [3] neutrinos. The typical L/E pattern expected for oscillations begins to emerge from various data sets like the most recent KamLAND data [4, 5] or the first generation of long-baseline ν_μ disappearance experiments K2K [6, 7] and MINOS [8]. The only experiment which cannot be accounted for in a three flavour oscillation framework is the LSND $\bar{\nu}_e$ appearance signal [9]. The LSND result is quite difficult to reconcile with the null results of CDHS [10] and Bugey [11], even when one allows for one or more sterile neutrinos. Recently, MiniBooNE failed to confirm the LSND signal [12]. For an analysis of sterile neutrino solutions to the LSND result in view of the MiniBooNE data see [13]. The status of LSND thus remains unclear and therefore we will assume that LSND has a non-oscillation explanation. We will consider only oscillations between three active flavours.

Neutrino oscillations require massive neutrinos. This on its own is one of the strongest and first indications for physics beyond the Standard Model. Most models for neutrino mass generation point to a very high energy scale far beyond the reach of current and future accelerator experiments. The neutrino is thus a unique messenger for otherwise in-accessible physics. To fully exploit this potential, new, high precision oscillation experiments are necessary. These experiments will address the size of θ_{13} , the neutrino mass hierarchy, leptonic CP violation and whether $\theta_{23} = \pi/4$. None of the currently running or approved experiments has sufficient sensitivity to achieve an accurate measurement of the neutrino mass hierarchy or CP violation [14]. The reason is, that in both cases the effects are quite small and subtle. There is a plethora of possible technologies to address these questions. They range from third generation superbeam experiments to beta beams and neutrino factories. For a recent review see [15].

In this paper we focus on third generation superbeam experiments. These experiments are based on conventional neutrino beams from π -decay. The experiments are ‘super’ in the sense that they will use proton beams of unprecedented strength around 1 – 4 MW and detectors with fiducial masses of several 100 kt. This will allow to collect many thousands of ν_e and $\bar{\nu}_e$ appearance events (assuming $\sin^2 2\theta_{13} = 0.1$). Thus statistical errors will be at most of percent size and systematical errors will be no longer be negligible. Nearly all previously published sensitivity studies use some *ad-hoc*¹ value of systematics which is assumed to be achieved by means of a near detector. This near detector is not specified nor included in the calculation.

In this paper we carefully investigate a large number of possible contributions to the systematical error budget in superbeam experiments. To be specific we use the T2K [16] experiment as example, focusing mainly on the discovery of CP violation in T2K phase II (T2HK). We briefly comment also on T2K phase I, as well as the T2KK proposal [17, 18], where half of the T2HK detector is moved to Korea. Our analysis is based on a realistic Monte Carlo study of the detector response and we explicitly include a (though somewhat idealised) near detector in the simulation. The goal of this paper is to investigate to which extent a near detector can contribute to reduce the impact of various systematical error sources. We will show that even an idealised near detector on its own cannot reduce the impact of all error terms. Thus additional information on fluxes and/or cross sections will be required.

The outline of the paper is as follows. In section 2 we discuss qualitatively the impact of systematics on an appearance experiment. Though highly simplified this discussion will allow us to understand many features of the numerical calculations. In section 3 we review in some detail uncertainties on neutrino cross sections, since they will be crucial in the subsequent analysis. In section 4 we give a brief description of our experiment simulation and the various types of systematics we include in our analysis. More technical details can be found in appendix A. Section 5 contains the results of our numerical calculations: in section 5.1 we consider the CP violation sensitivity of T2HK discussing mainly the impact of

¹*ad-hoc* refers to the fact that this value is usually smaller than any value achieved by any previous experiment.

cross section uncertainties, whereas in section 5.2 we point out under which circumstances information on fluxes and an improved near detector are useful. In section 5.3 we consider the determination of θ_{13} in the context of T2K (phase I) and T2HK (phase II), whereas in section 5.4 we discuss the systematics impact for T2KK in comparison with T2HK focusing again on CP violation. A summary and some speculative remarks on other high precision oscillation facilities follow in section 6. In appendix A.1 we give technical details on the experiment simulation, whereas in appendix A.2 we describe the statistical analysis including the implementation of systematics. In appendix B we show how the full ND/FD simulation can be approximated by a much simpler FD-only analysis adopting only very few “effective” systematics parameters.

2. Qualitative discussion

Before we plunge into a detailed numerical study, we will present here a simple argument, why even an idealised near detector is not sufficient for an appearance experiment. For the sake of discussion we introduce a couple of simplifications, for example we consider only total rates and neglect some background sources, while we do include them in the subsequent numerical calculations, see section 4 and appendix A for details.

The total number of ν_e and ν_μ events in near detector (ND) and far detector (FD) can be written as

$$n_{\nu_\mu}^{\text{ND}} = \frac{N_{\text{ND}}}{L_{\text{ND}}^2} \Phi_{\nu_\mu} \sigma_{\nu_\mu} \epsilon_{\nu_\mu} \quad (2.1)$$

$$n_{\nu_e}^{\text{ND}} = \frac{N_{\text{ND}}}{L_{\text{ND}}^2} [\Phi_{\nu_e} \sigma_{\nu_e} \epsilon_{\nu_e} + n_{\text{NC}}^{\text{ND}}] \quad (2.2)$$

$$n_{\nu_\mu}^{\text{FD}} = \frac{N_{\text{FD}}}{L_{\text{FD}}^2} \Phi_{\nu_\mu} P(\nu_\mu \rightarrow \nu_\mu) \sigma_{\nu_\mu} \epsilon_{\nu_\mu} \quad (2.3)$$

$$n_{\nu_e}^{\text{FD}} = n_{\nu_e}^{\text{FD,sig}} + n_{\nu_e}^{\text{FD,bg}} \quad (2.4)$$

with

$$n_{\nu_e}^{\text{FD,sig}} = \frac{N_{\text{FD}}}{L_{\text{FD}}^2} \Phi_{\nu_\mu} P(\nu_\mu \rightarrow \nu_e) \sigma_{\nu_e} \epsilon_{\nu_e}, \quad (2.5)$$

$$n_{\nu_e}^{\text{FD,bg}} = \frac{N_{\text{FD}}}{L_{\text{FD}}^2} [\Phi_{\nu_e} P(\nu_e \rightarrow \nu_e) \sigma_{\nu_e} \epsilon_{\nu_e} + n_{\text{NC}}^{\text{FD}}]. \quad (2.6)$$

Here N is the total normalisation (number of target nuclei), σ_{ν_α} is the charged current cross section for ν_α , ϵ_{ν_α} is the detection efficiency for ν_α (assumed to be identical for ND and FD), $P(\nu_\beta \rightarrow \nu_\alpha)$ is the probability for a neutrino of flavour β to oscillate into flavour α , Φ_{ν_β} is the initial neutrino flux, and L is the distance from the detector to the source. For the ν_e signal we include here the intrinsic ν_e beam contamination and the background from neutral current (NC) interactions $n_{\text{NC}} \times N/L^2$, whereas for the disappearance channel we neglect backgrounds. Note, that the efficiency ϵ and the cross section σ appear as product and hence we define an effective cross section

$$\tilde{\sigma}_{\nu_\alpha} := \sigma_{\nu_\alpha} \epsilon_{\nu_\alpha}. \quad (2.7)$$

Many of the quantities — most importantly cross sections and fluxes — appearing in eqs. (2.1) to (2.6) are subject to (sometimes large) uncertainties. Therefore, the aim is to use data from the ND in order to predict the signal in the FD, reducing the dependence on external information as much as possible. This can be done efficiently for a disappearance measurement. Using eqs. (2.1) and (2.3) one finds

$$n_{\nu_\mu}^{\text{FD}} = n_{\nu_\mu}^{\text{ND}} \frac{N_{\text{FD}}}{N_{\text{ND}}} \frac{L_{\text{ND}}^2}{L_{\text{FD}}^2} P(\nu_\mu \rightarrow \nu_\mu). \quad (2.8)$$

Hence, assuming that the uncertainty on $N_{\text{FD}}/N_{\text{ND}} \times L_{\text{ND}}^2/L_{\text{FD}}^2$ is negligible, a complete cancellation of all systematical errors happens (in this idealised discussion), since the same combination of $\tilde{\sigma}$ and Φ appears in ND and FD. This result is well known and has been exploited with success in the K2K [6] and MINOS [8] experiments.² Also, it is the basis for all of the latest generation of reactor neutrino experiments like DoubleChooz [19, 20]. For reactor experiments, the idea is that by careful design and construction, the near to far comparison can be made so precise that eq. (2.8) holds to an accuracy of better than 1%.³

However, the situation is very different for an appearance experiment. Depending on the relative importance of the two terms in eq. (2.4) we can identify two qualitatively different regimes for the appearance measurement: first, the regime close to the sensitivity limit of the experiment (i.e., small $\sin^2 2\theta_{13}$), where the ν_e events are dominated by background, and second, the regime of large $\sin^2 2\theta_{13}$, where the actual appearance signal dominates over the background in eq. (2.4). Hence, depending on the regime, one expects that either the error on the background or on the signal is most relevant for the sensitivity. As the numerical calculations will show, for T2HK the transition between the two regimes occurs roughly at $\sin^2 2\theta_{13} \simeq 0.01$.

In the background dominated case of small $\sin^2 2\theta_{13}$ the ND plays a crucial role in measuring the background. Under the assumption that the NC background is the same in ND and FD, and neglecting the small effect of oscillations on the beam background, $P(\nu_e \rightarrow \nu_e) \approx 1$, the background in the FD can be predicted by the ν_e events in the ND from eq. (2.2):

$$n_{\nu_e}^{\text{FD,bg}} = n_{\nu_e}^{\text{ND}} \frac{N_{\text{FD}}}{N_{\text{ND}}} \frac{L_{\text{ND}}^2}{L_{\text{FD}}^2}. \quad (2.9)$$

It becomes important how well the above assumptions are fulfilled, for example, how well one can extrapolate the NC background from ND to FD. Moreover, the statistical precision for $n_{\nu_e}^{\text{ND}}$ is an issue, i.e., the size of the ND, since the beam contains only a small component of ν_e , at the level of 1% of ν_μ . Note that in the discussion leading to eq. (2.9) we have neglected a background coming from ν_μ charged-current interactions. This background is

²Certainly, in real life the situation is much more complicated than suggested by eq. (2.8) which should illustrate the principle. In the K2K and MINOS analyses many additional complications have been taken into account. For example, in both cases the fluxes are rather different in ND and FD, and effects of the energy spectrum are included via a near-to-far extrapolation matrix.

³For reactor experiments, this very high accuracy is possible because the fiducial mass will be determined within less than 0.5%. Moreover, the efficiencies are close to 100%, hence there will be only a very small error due to event reconstruction.

very different in ND and FD because of oscillations of ν_μ with $\sin^2 2\theta_{23} \simeq 1$. Therefore, this additional background component will further complicate the extrapolation of the background measurement from the ND to the FD. While we neglect such a background in the current section for simplicity, we do include a background from μ/e miss-identification in the numerical calculations, see section 4.

The signal dominated regime of large $\sin^2 2\theta_{13}$ is probably the more interesting case, since it will allow for high precision measurements such as CP violation (CPV), and therefore the main focus of our work is on this case. From eq. (2.5) one can see that for the signal the combination $\Phi_{\nu_\mu} \times \tilde{\sigma}_{\nu_e}$ is relevant, which cannot be determined by the ND, and eqs. (2.1) and (2.5) combine to

$$n_{\nu_e}^{\text{FD,sig}} = n_{\nu_\mu}^{\text{ND}} \frac{N_{\text{FD}}}{N_{\text{ND}}} \frac{L_{\text{ND}}^2}{L_{\text{FD}}^2} \frac{\tilde{\sigma}_{\nu_e}}{\tilde{\sigma}_{\nu_\mu}} P(\nu_\mu \rightarrow \nu_e). \quad (2.10)$$

Obviously, there remains some dependence on the effective cross sections, namely the ratio $\tilde{\sigma}_{\nu_e}/\tilde{\sigma}_{\nu_\mu}$ survives. The ability to discover CPV largely depends on the ability to compare the neutrino and anti-neutrino appearance signals, thus it is useful to look at the ratio of the corresponding event rates:

$$\frac{n_{\nu_e}^{\text{FD,sig}}}{n_{\bar{\nu}_e}^{\text{FD,sig}}} = \frac{n_{\nu_\mu}^{\text{ND}}}{n_{\bar{\nu}_\mu}^{\text{ND}}} \frac{\tilde{\sigma}_{\nu_e}}{\tilde{\sigma}_{\nu_\mu}} \frac{\tilde{\sigma}_{\bar{\nu}_\mu}}{\tilde{\sigma}_{\bar{\nu}_e}} \frac{P(\nu_\mu \rightarrow \nu_e)}{P(\bar{\nu}_\mu \rightarrow \bar{\nu}_e)}. \quad (2.11)$$

From this discussion we learn that one of the following combinations of quantities has to be known in order to predict the signal for the CPV measurement:

$$\left(\frac{\tilde{\sigma}_{\nu_e}}{\tilde{\sigma}_{\nu_\mu}}, \frac{\tilde{\sigma}_{\bar{\nu}_e}}{\tilde{\sigma}_{\bar{\nu}_\mu}} \right) \quad \text{or} \quad \left(\frac{\tilde{\sigma}_{\nu_e}}{\tilde{\sigma}_{\bar{\nu}_e}}, \frac{\tilde{\sigma}_{\nu_\mu}}{\tilde{\sigma}_{\bar{\nu}_\mu}} \right) \quad \text{or} \quad \left(\frac{\Phi_{\nu_\mu}}{\Phi_{\bar{\nu}_\mu}}, \frac{\tilde{\sigma}_{\nu_e}}{\tilde{\sigma}_{\bar{\nu}_e}} \right). \quad (2.12)$$

The first two combinations follow from eq. (2.11): if either the flavour ratio of effective cross sections for neutrino and anti-neutrinos separately or the neutrino/anti-neutrino ratio for ν_e and ν_μ separately are known with good precision then the high statistics ν_μ and $\bar{\nu}_\mu$ samples from the ND allow to predict the CPV signal in the FD. Note that this does not require knowledge on the double ratio $(\tilde{\sigma}_{\nu_e}/\tilde{\sigma}_{\nu_\mu})/(\tilde{\sigma}_{\bar{\nu}_e}/\tilde{\sigma}_{\bar{\nu}_\mu})$. The last combination in eq. (2.12) follows directly from eq. (2.5): If ν_μ and $\bar{\nu}_\mu$ fluxes, as well as ν_e and $\bar{\nu}_e$ effective cross sections are known the signal can directly be predicted without the need of the ND. Let us mention again that in eq. (2.12) always the product of cross sections times efficiencies appears. Uncertainties on both of them contribute to the error on $\tilde{\sigma}$. Although the preceding discussion is highly simplified it captures quite well the behaviour of the near/far detector system for an appearance experiment. Many results of our numerical simulation can be understood qualitatively with this kind of reasoning, and in the course of our discussion we will refer frequently to the arguments presented in this section. In appendix B we demonstrate that these arguments can be used to approximate the full ND/FD simulation by a rather simple (in what concerns the systematics treatment) FD-only setup.

3. Neutrino cross sections

Since cross section ratios play such an important role in the discussion of systematics, we would like to make a few remarks. Based purely on existing experimental data [21], without

the use of a specific model, the errors are in the range 20 – 50%. Especially anti-neutrino cross sections are not well measured or for some energy ranges not measured at all. T2HK operates in the energy range from 400 – 1200 MeV, therefore most events (at least after the single ring cut) will be due to quasi-elastic (QE) reactions and we will focus on these. The theory for neutrino scattering off a free nucleon is well understood [22]. Here the cross section is given as a function of various form factors,⁴ which are all but one well measured. The one ‘free’ parameter is the axial mass m_A . Based on that formulation, one would expect that the ratio of σ_{ν_e} to σ_{ν_μ} can be accurately computed. However, in most detectors the bulk of the fiducial mass stems from heavier nuclei, therefore nuclear effects are non-negligible. Many experiments use the Smith-Moniz formalism [24] to account for nuclear effects. Here, the nucleus is described as a Fermi gas of nucleons and two new parameters enter: the Fermi momentum k_F and the binding energy E_B . This description thus introduces a smearing of the energy of the outgoing neutrino due to Fermi motion and a reduction of the cross section due to Pauli blocking. There are basically two differences between electron and muon neutrino scattering: one is the pure kinematic effect of the difference in m_e and m_μ . This effect is trivial to account for. The other one is, the fact the momentum transfer to the nucleus is going to be different. In order to compute the resulting effect on the ratio it is necessary to know the momentum distribution of the bound nucleon.

Moreover, it is not clear how well the Fermi gas model actually captures the physics of the interaction of a neutrino with bound nucleons. Until recently the consensus value for the axial mass was $m_A = 1.025 \pm 0.021$ GeV [25]. This is somewhat in contrast with values reported by K2K [26] of $m_A = 1.20 \pm 0.12$ GeV and MiniBooNE [27] of $m_A = 1.23 \pm 0.20$ GeV. One possible explanation, put forth in [27], is that the old data was mainly obtained on Deuterium, where nuclear effects are very small, whereas the new data used Oxygen (K2K) or Carbon (MiniBooNE). This in turn would indicate that there are nuclear effects which are not properly included in the Smith-Moniz formalism and thus the value of m_A determined from nuclei is in reality an effective parameter. However, it was pointed out in [23] that m_A should be the same or decrease in a nuclear target compared to deuterium, see also [28]. Thus the experimental situation on the quasi-elastic cross section itself is somewhat unclear. It may be that the data on which the value for m_A in [25] is based are not pure QE events, which of course would introduce a bias into the determination of m_A . The value of m_A itself is not expected to have a large impact on the ratio of cross sections. This example is intended to show that there are still open issues in seemingly well understood neutrino interaction processes. Also a comparison of several state of art event generator in the range $0 < E_\nu < 2$ GeV yields errors in the range 5%–15% [29].

Clearly, from a purely theoretical point of view any correction due to finite lepton masses should be small especially for energies $E \gg m_\mu$, which is the case for T2HK. Surprisingly we found only very little literature discussing the cross section ratio. There are many papers computing either the ν_μ or ν_e QE cross section on various nuclei, but only in refs. [30–32] we could find a result for both, ν_μ and ν_e on Oxygen.⁵ In ref. [31] the

⁴There are some deviations from pure dipole form, which, however, can be accounted for, see *e.g.* [23].

⁵We do not claim that our survey is complete, but it certainly is representative of the small number of

error on the ratio is quantified explicitly, however only in the energy range below 500 MeV. Their result is, that within the model given in [33] the errors are about 1% coming from the uncertainties of the input parameters. They also estimate that physical effects not accounted for introduce no more than 5% error on the ratio. Ref. [32] gives both cross sections in the energy range relevant for T2HK. The authors of [32] kindly provided their results and we could compute the ratio and compare it to the results in [33]. At 450 MeV we find a difference in the ratios of about 3%, which falls within the error estimate given in [33].

We furthermore compared the results for the ratio obtained with the event generators NUANCE [34], GENIE [35] and NEUGEN [36] and we find between 400 – 1200 MeV a spread of about 1%.⁶ With respect to the theoretical calculation in [32] we find a difference of 3% at 400 MeV which decreases down to 0.5% at 1200 MeV. We extracted the data in [30, 31] from the published plots and, within the errors this inevitably introduces, they show a similar spread. Summarising, all theoretical sources for the ratio we could find, showed a spread of 3% or less throughout the energy range relevant for T2HK. Let us mention that in the energy region of a few 100 MeV, the error on the ratio from theory reaches more than 10%. This energy range is relevant for a beta beam with a Lorentz- γ of around 100 or the SPL superbeam [37]. Therefore, in these cases present theory calculations do not provide a relevant constraint on the ratio. Also note, that the spread for the ratio of neutrino to anti-neutrino cross sections is found to be larger than 10% throughout the whole energy range for T2HK.

MiniBooNE offers an excellent case study of how a recent experiment deals with these issues. MiniBooNE is a ν_e appearance experiment in the same energy region than T2HK, which uses, instead of a near detector, the unoscillated ν_μ sample in the far detector to predict their ν_e backgrounds and also the ν_e signal. A dedicated investigation of the effect of cross section uncertainties has been performed, and the results of ref. [38] indicate that the ν_μ to ν_e cross section ratio has an error of about 8 – 9%.

The question is, whether one trusts theory calculations, which state that the ratio is known to better than 3%. If this is the case, the cross section ratio would have only a small impact on the overall error budget and the near-far comparison would effectively control the systematics also in an appearance experiment. On the other hand, one should acknowledge the fact that neutrino scattering data is sparse and no theory of quasi-elastic scattering has been experimentally tested with a large degree of accuracy. Thus there is, at least in principle, considerable room for surprises and consensus is needed on whether this risk is tolerable in view of a large scale project such as considered here. For instance, there is a long standing excess of ν_e events in sub-GeV atmospheric neutrino data [3], whose origin so far is not understood and might reflect a problem in the ν_e/ν_μ cross section ratio.⁷ Also, the error estimate obtained by MiniBooNE clearly points towards much larger errors of the order 10%, than our survey of theory results has found.

Summarising, it seems that the 10% default errors used here for the individual cross

pertinent results compared to the total amount of literature about neutrino cross sections.

⁶NEUGEN and GENIE give nearly identical results.

⁷We thank E. Lisi for pointing this out.

sections are somewhat optimistic, especially if one keeps in mind that basically all existing data is nearly exclusively for ν_μ . On the other hand, with our defaults and assumption of uncorrelated errors for all cross sections, the ratio $\sigma_{\nu_e}/\sigma_{\nu_\mu}$ would have an effective error of $\sim 10\%$ (see appendix B), which may be larger than expected from theory but is in agreement with the MiniBooNE numbers. In the following we will take the conservative view point, that we would like to be independent of theoretical arguments about the cross section ratio and use (by then) available experimental data to control systematical uncertainties. Nonetheless, we show results for various constraints on this ratio. Note, that the error relevant for the oscillation analysis is the error on the ratio of the product of cross section and efficiency. Thus, even if there is a tight constraint on the cross section ratios, the efficiencies still will need to be determined accurately by other means.

4. Description of the simulation

Let us now give some key features of our numerical simulation. More technical details are deferred to appendix A. We consider the following standard setup for the phase I (phase II) T2K (T2HK) configuration. The fiducial far detector mass is 22.5 kt (500 kt) and the beam power is 0.77 MW (4 MW). The running time is for T2K and T2HK 2 yr for the neutrino and 6 yr for the anti-neutrino beams. The baseline is 295 km and we use an average matter density of 2.8 g cm^{-3} . This setup is based on [16]. Details of the T2KK setup are given in section 5.4. We consider the signals from ν_μ and ν_e single ring events, for both the neutrino and anti-neutrino run, i.e., disappearance and appearance channels, and we take into account also the effect of oscillations on various background components. Energy resolution is treated with migration matrices including nuclear effects as well as the contamination of the single ring sample with non-quasi-elastic events. We include the intrinsic ν_e , $\bar{\nu}_e$ and $\bar{\nu}_\mu$ (and the CP conjugate ones for the anti-neutrino run) as well as neutral current backgrounds. We restrict the analysis to reconstructed neutrino energies from 0.4 – 1.2 GeV. This range is divided into 8 equidistant bins. For the near detector we assume a water Čerenkov detector with fiducial mass of 0.1 kt and otherwise identical properties to the far detector. Specifically, we also assume the same acceptance, i.e. a flat near-far ratio. This assumption translates into the requirement that the near detector distance must be large enough in order to see the decay pipe as point source like the far detector. To be specific, we follow the choice of the T2K collaboration and use a baseline of 2 km for the near detector [39]. Further details on the detector simulation are to be found in appendix A.

The χ^2 computation is based on a standard Poissonian form and we use the so-called pull approach [40, 41] to include the various sources of systematical errors. For the implementation of the systematical errors and an explicit definition of the χ^2 -function see appendix A.2. The calculations have been performed with the GLoBES software [42–44], exploring the possibility of user-defined χ^2 in order to include the various systematics with the proper correlations. A GLoBES glb-file for our T2HK simulation with an effective systematics treatment (see appendix B) is available at [44].

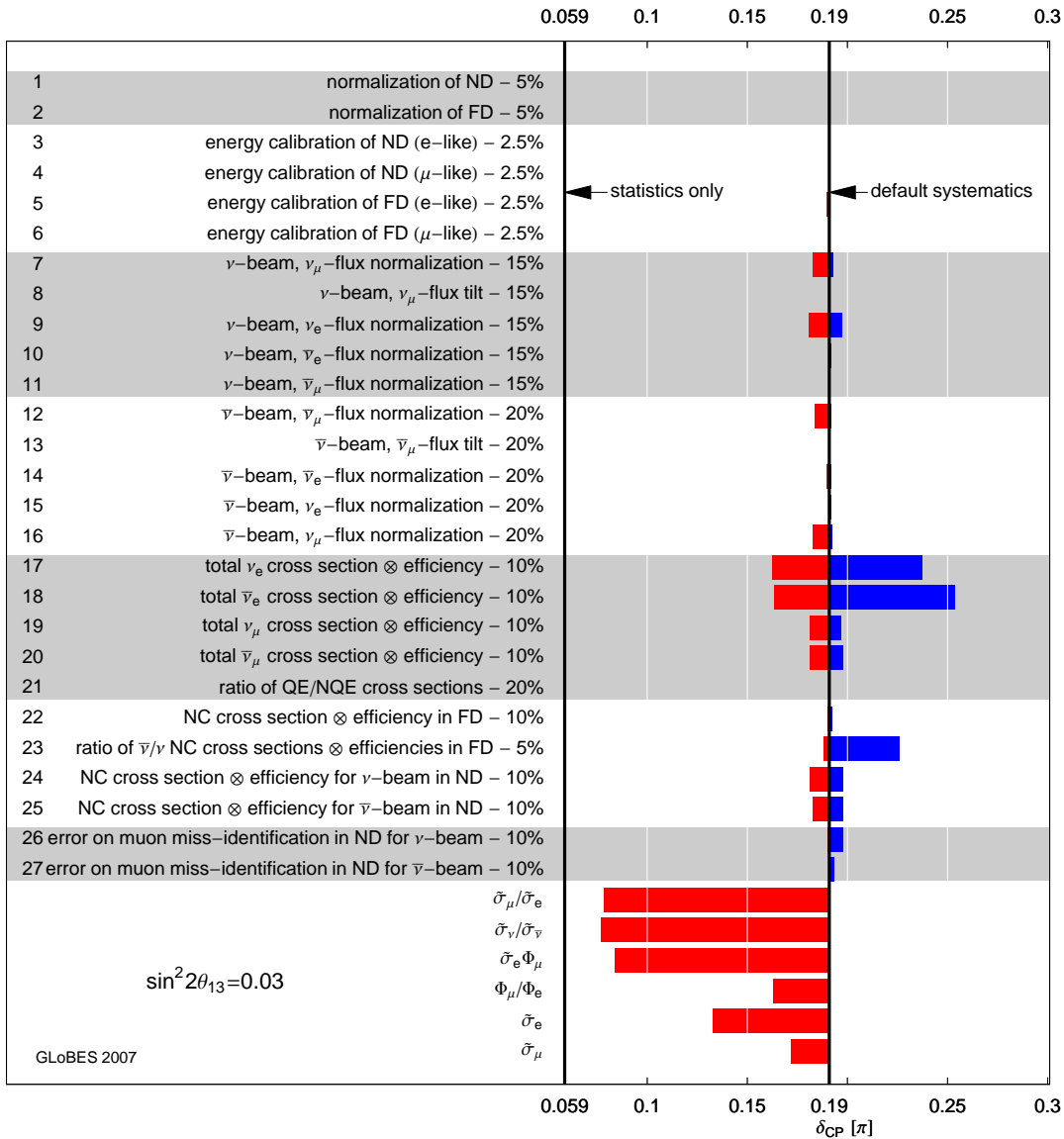


Figure 1: List of the systematical uncertainties and the adopted default values, as well as the impact of various systematics on the T2HK sensitivity to CPV for $\sin^2 2\theta_{13} = 0.03$. The abscissa shows the smallest δ_{CP} in $[0, \pi/2]$ for which CPV can be established at 3σ . We show how the sensitivity is affected if each of the 27 pulls is switched off (red) or the error is multiplied by 5 (blue). The lower 6 rows show the impact when certain combinations of pulls are constrained at 2%: the ratio of ν_e to ν_μ cross sections times efficiencies (for neutrinos and anti-neutrinos), the ratio of neutrino and anti-neutrino cross sections times efficiencies (for e and μ -like events), the product of ν_μ flux times ν_e cross section times ν_e efficiency (for neutrinos and anti-neutrinos), the ratio of e to μ fluxes (for neutrinos and anti-neutrinos), ν_e and $\bar{\nu}_e$ cross sections times efficiencies, ν_μ and $\bar{\nu}_\mu$ cross sections times efficiencies.

We include 27 uncorrelated errors listed in figure 1 together with the adopted default values. They include detector normalisations and energy calibration errors, uncertainties on the initial fluxes, cross section uncertainties which in our convention include also uncertain-

ties on the efficiencies, as well as errors on NC backgrounds and muon miss-identification. A more detailed discussion is given in appendix A.2 including also some motivations for our default values. We stress that our defaults should by no means be considered as the most realistic values, especially at the time when the experiment is actually performed. Our assumptions are motivated by the present situation (see appendix for references) or in other cases are very conservative guesses. The purpose of our work is not to advocate specific values for the systematics. Instead we want to identify the crucial uncertainties which cannot be eliminated with the help of the ND, and hence, for which solid external information is required.

5. Results

5.1 CP violation at T2HK

In figure 2 we show the 3σ sensitivity of T2HK for CPV. We restrict the analysis to the range $0 \leq \delta_{\text{CP}}^{\text{true}} \leq \pi/2$, and we neglect the $\text{sign}(\Delta m_{31}^2)$ degeneracy. When calculating the χ^2 for $\delta_{\text{CP}} = 0$ and π we fix all oscillation parameters except from θ_{13} to their assumed true values $\Delta m_{31}^2 = 2.4 \times 10^{-3} \text{ eV}^2$, $\sin^2 \theta_{23} = 0.5$, $\Delta m_{21}^2 = 7.9 \times 10^{-5} \text{ eV}^2$, $\sin^2 \theta_{12} = 0.3$. This allows to focus exclusively on the impact of systematics for the discovery of CPV.⁸ The figure shows the sensitivity from statistical errors only (lower black curve), which is obtained by fixing all 27 systematic pulls to zero, as well as the sensitivity for our default choice of systematical errors according to figure 1 (upper black curve). Clearly the impact is rather dramatic for large θ_{13} , in the region $\sin^2 2\theta_{13} \gtrsim 10^{-2}$. The effect of the various systematics in that region is illustrated in figure 1, where we show what happens to the smallest δ_{CP} for which CPV can be established at 3σ if each single pull is switched off one by one (red bars) or multiplied by a factor of 5 (blue bars), assuming $\sin^2 2\theta_{13} = 0.03$. No single pull has a large impact on its own, which highlights the importance of a comprehensive treatment of a large number of possible error sources.

In figure 2 we show the case when rather precise information (a hypothetical 1% error) is available for either the ν_μ and $\bar{\nu}_\mu$ effective cross sections or the ν_e and $\bar{\nu}_e$ effective cross sections. Future cross section experiments such as e.g. MINER ν A [45] or SciBooNE [46] aim for a 5% accuracy on the absolute ν_μ cross section. In section 5.2 we explore under which circumstances the near detector itself can perform an accurate cross section measurement. Note, that the effective cross section is defined as the product of cross section and efficiency. Therefore, also the efficiencies would have to be known to better than 1%. Apparently only a marginal improvement is possible for precisely known ν_μ effective cross sections. This is not very surprising since for ν_μ the near detector can indeed cancel a large fraction of the associated errors. Knowing the ν_e effective cross section would be helpful (c.f. also figure 1), since here the near detector provides very limited information, and the signal is directly proportional to this cross section. However, clearly this information alone cannot resolve the bulk of the systematics problem.

⁸For the sensitivity to CPV as shown in figure 2 the impact of the uncertainty on the oscillation parameters (as well as on the matter density) is negligible. See also the discussion later in connection with figure 8.

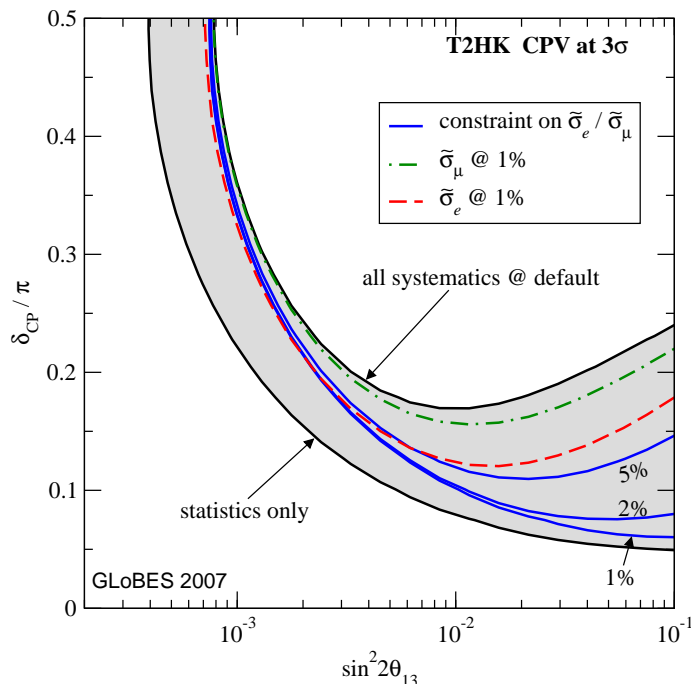


Figure 2: T2HK CPV sensitivity at 3σ for our default choice of systematical errors according to figure 1 and for statistical errors only (curves delimiting the shaded region). We show also the sensitivity if certain constraints on the product of cross sections times efficiencies $\tilde{\sigma}$ are available: 1% accuracies on $\tilde{\sigma}_{\nu_e}$ and $\tilde{\sigma}_{\nu_\mu}$ for neutrinos and anti-neutrinos, and 5%, 2%, 1% accuracies on the ratios $\tilde{\sigma}_{\nu_e}/\tilde{\sigma}_{\nu_\mu}$ for neutrinos and anti-neutrinos.

In contrast, the situation improves significantly if external information is available on the ratio of the effective cross sections $\tilde{\sigma}_R \equiv \tilde{\sigma}_{\nu_e}/\tilde{\sigma}_{\nu_\mu}$ for neutrinos and anti-neutrinos. Such information can come either from theoretical calculations (for the cross section only, see section 3) or dedicated experiments. In order to perform this analysis we take into account a correlation matrix between the pulls corresponding to the effective cross sections, which imposes a constraint on the ratio. Hence, we replace the uncorrelated penalty terms for the pulls in eq. (A.3) by a matrix correlating the relevant pulls. In figure 2 curves are shown corresponding to an error on $\tilde{\sigma}_R$ of 5%, 2% and 1%. Clearly, at the largest values of θ_{13} the error budget is dominated by $\tilde{\sigma}_R$, and constraining this quantity basically would allow to recover most of the statistical accuracy of the experiment. This is in agreement with the discussion in section 2, and can be understood by the fact the relative size of CP effects is smallest for large θ_{13} and hence the absolute accuracy of the prediction of the number of oscillated ν_e events becomes very important. Any CP effect has to be uncovered from this number or, more precisely, from its error. The contribution of backgrounds to the number of ν_e events is small and the contribution to the error is even smaller. The effect of a constraint on $\tilde{\sigma}_R$ is also shown in the lower part of figure 1, where we show the impact of constraining certain combinations of systematics. There we display also the impact of a constraint on the ratio of effective neutrino and anti-neutrino cross sections, which has a very similar effect as a constraint on the flavour ratio (even slightly more effective) for restoring the

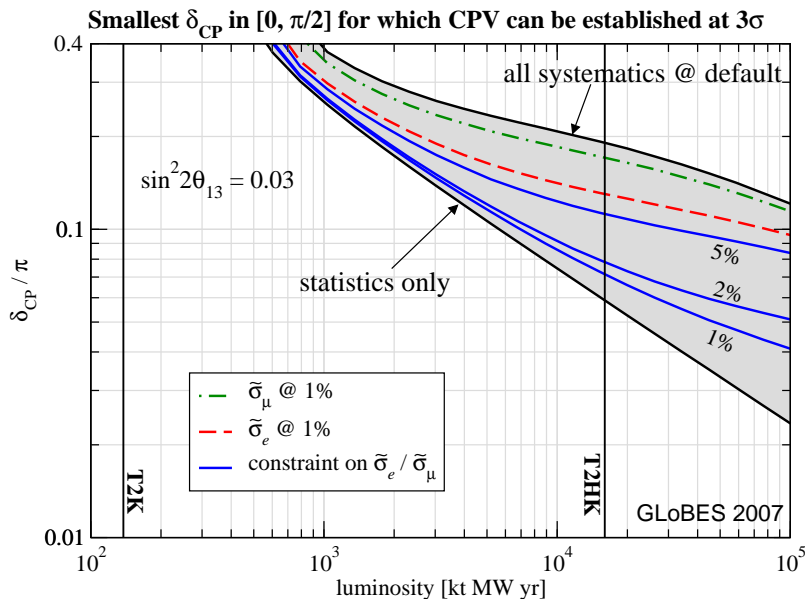


Figure 3: CPV sensitivity at 3σ as a function of exposure for a true value $\sin^2 2\theta_{13} = 0.03$ for our default choice of systematical errors according to figure 1 and for statistical errors only (curves delimiting the shaded region). The ratio of neutrino to anti-neutrino running is kept constant at 1 : 3. Furthermore we show the sensitivity if certain constraints on the product of cross sections times efficiencies $\tilde{\sigma}$ are available: 1% accuracies on $\tilde{\sigma}_{\nu_e}$ and $\tilde{\sigma}_{\nu_\mu}$ for neutrinos and anti-neutrinos, and 5%, 2%, 1% accuracies on the ratios $\tilde{\sigma}_{\nu_e}/\tilde{\sigma}_{\nu_\mu}$ for neutrinos and anti-neutrinos.

statistics-only sensitivity, in agreement with the discussion related to eq. (2.12).

Figure 3 shows the luminosity scaling of the sensitivity to CPV in the region of large θ_{13} ($\sin^2 2\theta_{13} = 0.03$) with the same set of curves as in figure 2. For this analysis we scale simultaneously the beam power and the FD mass between the T2K (0.77 MW, 22.5 kt) and T2HK (4 MW, 500 kt) benchmarks defined in section 4, and we always assume a neutrino (anti-neutrino) running time of 2 (6) years, and hence a factor 8 yr is included in the horizontal axis in figure 3. The ND mass is fixed at 0.1 kt. Obviously, the impact of systematics becomes larger as the luminosity increases. Increasing luminosity is a possibility to compensate for systematical errors, though a very costly one. For example, if an external constraint on the ratio $\tilde{\sigma}_{\nu_e}/\tilde{\sigma}_{\nu_\mu}$ at 2% were available T2HK could have 1/10 of the luminosity and still achieve the same sensitivity to CPV as in the default configuration. Thus, any optimised experimental strategy has to find the right balance between spending on measures to mitigate systematical effects and on maximising the total luminosity. This may require a dedicated effort since some of the necessary measurements may be external to the actual oscillation experiment.

Let us briefly comment on the region of small θ_{13} close to the sensitivity limit. Figure 2 shows that in this case a constraint on $\tilde{\sigma}_{\nu_e}/\tilde{\sigma}_{\nu_\mu}$ cannot reduce the effect of systematics. The reason is that in this region the precision on the background determines the sensitivity, see the discussion in section 2. This leads to rather different requirements than in the region of large θ_{13} . The relevant question is here to which accuracy the ND data can be used to

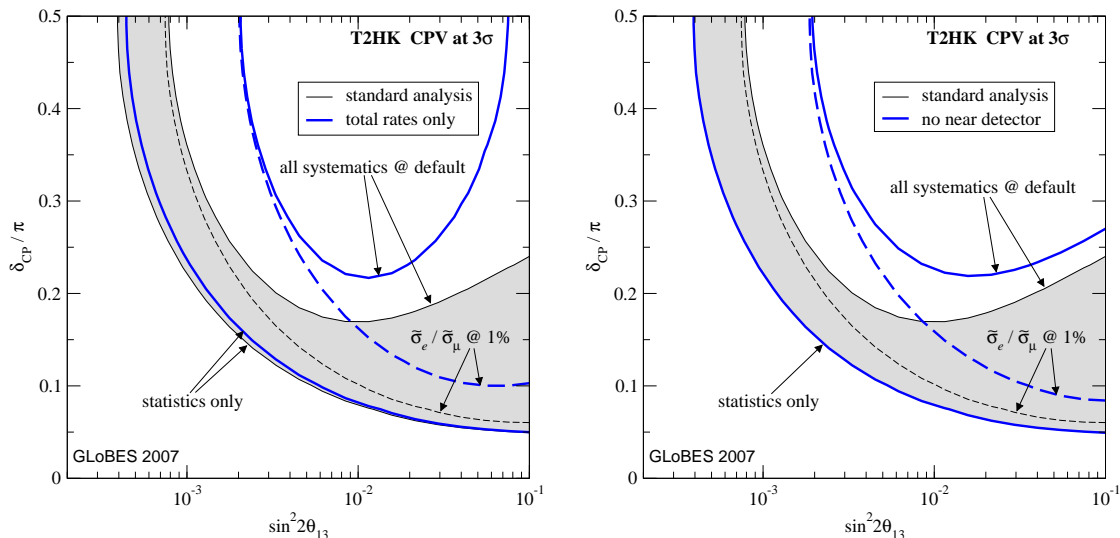


Figure 4: T2HK CPV sensitivity at 3σ for a total rate measurement only (left) and without a near detector (right) for our default choice of systematical errors according to figure 1 and for statistical errors only. The dashed curves correspond to an external accuracy of 1% on the ratios $\tilde{\sigma}_{\nu_e}/\tilde{\sigma}_{\nu_\mu}$ for neutrinos and anti-neutrinos. The shaded regions correspond to our standard analysis and are identical to the one in figure 2.

predict the background in the FD, c.f. eq. (2.9). This ability is limited by backgrounds in the ND (*e.g.*, NC, muon miss-identification), as well as by statistics in the ND.

Figure 4 (left) shows the impact of spectral information. The first observation is that the pure statistics sensitivity hardly changes if only rate information is used, which shows that the main oscillation physics is captured just in the total number of events.⁹ However, the spectrum is important to disentangle oscillation effects from systematics, especially in the regions of very small θ_{13} (to measure the background in the ND) and very large θ_{13} (to avoid confusion of the CPV signal with systematics). This result indicates that the systematics question in the context of a wide band beam [47–49] might be different, and it would be desirable to have a similar analysis also for such a facility.

In figure 4 (right) we show the sensitivity to CPV without any near detector. This plot highlights the importance of the ND for small θ_{13} , where it is needed to constrain the background. However, the impact of the ND is somewhat smaller for large θ_{13} , $\sin^2 2\theta_{13} \gtrsim 0.05$, since here the question of backgrounds is less important, whereas the main uncertainty comes from the combinations given in eq. (2.12), *e.g.* the ratio $\tilde{\sigma}_{\nu_e}/\tilde{\sigma}_{\nu_\mu}$, for which the ND provides only rather poor constraints.

5.2 Constraints on neutrino fluxes and properties of the near detector

Let us now discuss the impact of some external knowledge on the initial neutrino fluxes. In this case some of our default values might appear slightly too conservative. Information

⁹Note that spectral information is crucial for resolving the so-called intrinsic degeneracy, see *e.g.* [40, 17, 37]. However, since the intrinsic degeneracy does not confuse CP violating and conserving values of δ_{CP} it does not affect the sensitivity to CP violation shown in figure 4.

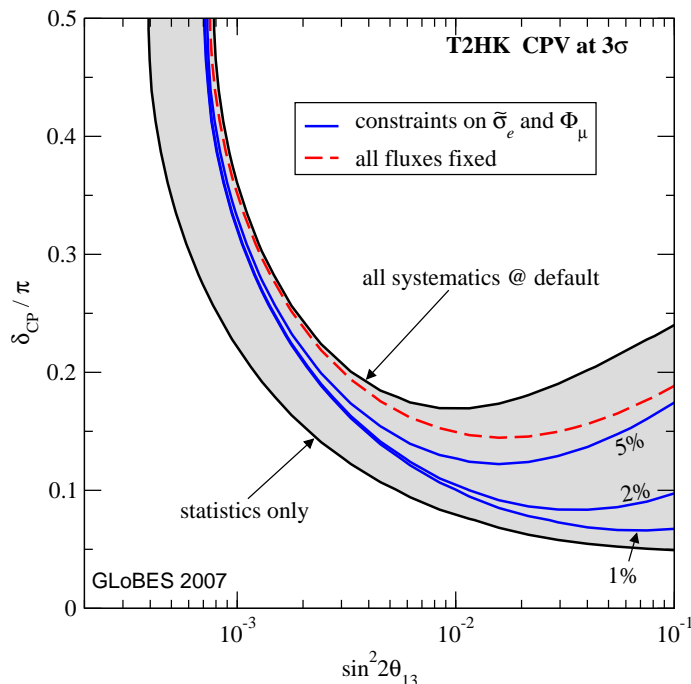


Figure 5: T2HK CPV sensitivity at 3σ . We show the impact of perfectly known fluxes, as well as constraints at 5%, 2%, 1% on $\tilde{\sigma}_{\nu_e}$ and ν_μ fluxes, both for neutrinos and anti-neutrinos. The shaded region corresponds to our standard analysis and is identical to the one in figure 2.

on the fluxes requires careful instrumentation of the beam line and data from dedicated Hadron production experiments such as MIPP [50] in the case of MINOS, HARP [51, 52] for K2K and MiniBooNE, or NA61/SHINE [53] for T2K. For example, in MINOS the goal is to constrain Φ_{ν_μ} at the 5% level using MIPP data. It is beyond the scope of this work to do a detailed study of how well neutrino fluxes can ultimately be determined. Here we investigate the case of perfectly well known fluxes and how useful that would be for the CPV measurement in T2HK.

The dashed curve in figure 5 corresponds to the case of perfectly known fluxes (including all sub-dominant flavours in each beam) with all other systematics at the default values. The sensitivity improves slightly for $\sin^2 2\theta_{13} \gtrsim 0.01$, but clearly this information is not enough to significantly address the systematics problem. The reason can again be understood from the discussion in section 2. Eq. (2.10) shows that the uncertainty on $\tilde{\sigma}_{\nu_e}/\tilde{\sigma}_{\nu_\mu}$ remains, irrespectively of the uncertainty on the fluxes. As mentioned in the paragraph after eq. (2.12) flux information is only useful in combination with a constraint on the effective ν_e cross section. This is confirmed by the blue curves in figure 5, which show that the impact of systematics can efficiently be reduced by accurate external information on both, Φ_{ν_μ} and $\tilde{\sigma}_{\nu_e}$ (for neutrinos and anti-neutrinos). Note that this information is not provided by the ND, but has to come from sources outside the considered setup. This seems especially difficult for ν_e and $\bar{\nu}_e$ cross sections.

Let us elaborate more on the somewhat surprising result, that knowing the fluxes has such a small impact. Indeed, in this case one may expect that the ND should be able to

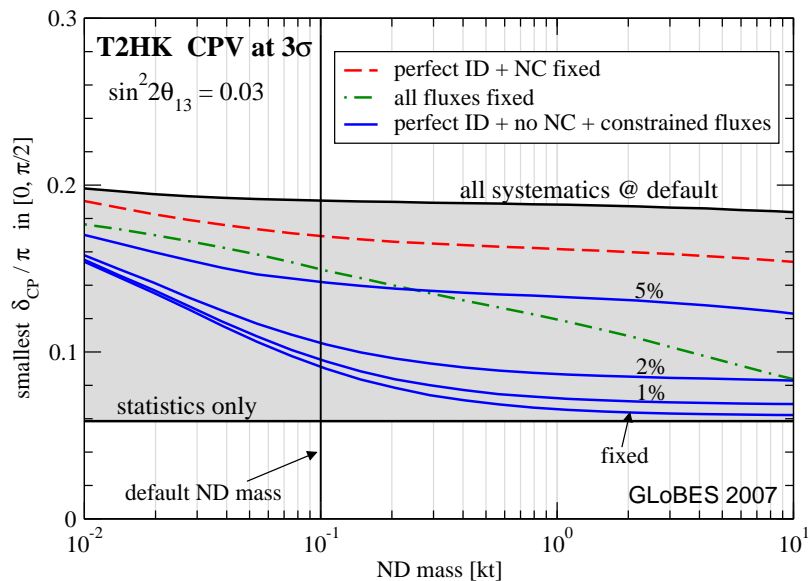


Figure 6: CPV sensitivity at 3σ for T2HK as a function of the near detector mass for a true value $\sin^2 2\theta_{13} = 0.03$ for our default choice of systematical errors according to figure 1 and for statistical errors only (curves delimiting the shaded region). The red/dashed curve corresponds to a ND with perfect e/μ separation and with perfectly known NC background, but all other systematics at default. The green/dash-dotted curve corresponds to the standard ND but we assume that all fluxes are perfectly known. For the blue/solid curves we assume a ND with perfect e/μ separation and without any NC background plus some knowledge on the fluxes according to the labels.

provide a measurement of $\tilde{\sigma}_{\nu_e}$ via the intrinsic ν_e component in the beam (which is assumed to be known perfectly). This argument is true in principle, however, we find that within our implementation the NC background and the muon miss-identification in the ND plus statistical errors in the ND are enough to spoil this measurement. We illustrate this effect in figure 6 by showing the CPV sensitivity for $\sin^2 2\theta_{13} = 0.03$ as a function of the ND mass, while keeping our T2HK default values for beam power, FD mass, and $\nu/\bar{\nu}$ running times constant. First, we note that for all systematics at default the sensitivity depends very little on the size of the ND, which is consistent with figure 4 (right). Second, the curve for known fluxes (green/dash-dotted) shows a modest gain in sensitivity at the default ND mass of 0.1 kt from figure 5, and some improvement with increasing the mass. However, the situation clearly improves if a “perfect” ND without muon miss-identification and NC background is assumed. In this case it only depends on the statistical errors in the ND and on the a priori accuracy of the fluxes, how well $\tilde{\sigma}_{\nu_e}$ can be determined by the ND. This can be seen from the blue/solid curves in figure 6, corresponding to a “perfect” ND plus a constraint on the fluxes, where the accuracy indicated in the figure is implemented as an uncorrelated error on each of the flux components. From the plot we find that for a flux uncertainty of 1% the pure statistics sensitivity is nearly reached for ND masses of about 1 kt. Let us add that such a “perfect” ND would also improve the sensitivity to CPV at small θ_{13} , since it would provide an accurate determination of the background.

To summarise this discussion, if precise information on fluxes is available (including

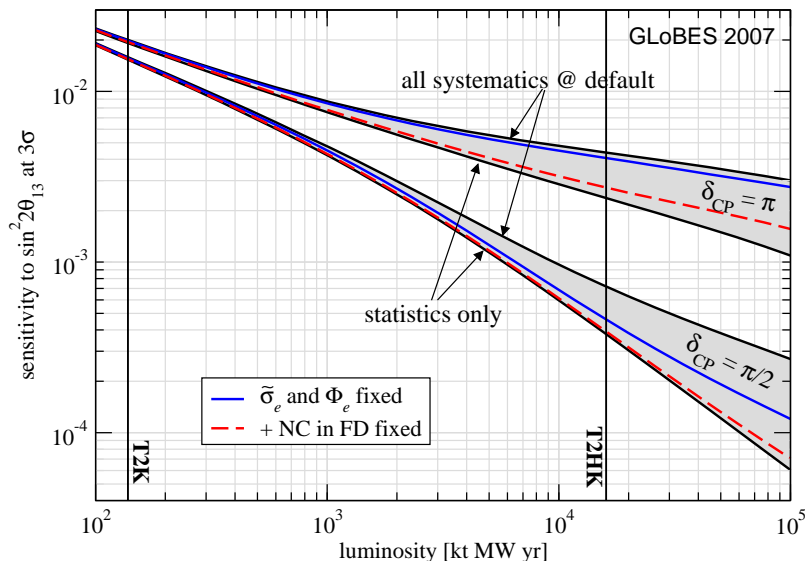


Figure 7: Sensitivity at 3σ to a non-zero θ_{13} as a function of exposure for $\delta_{CP} = \pi/2$ and π for our default choice of systematical errors according to figure 1 and for statistical errors only (curves delimiting the shaded region). The ratio of neutrino to anti-neutrino running is kept constant at 1 : 3. Furthermore, we show the sensitivity obtained without uncertainty on the intrinsic beam background (by fixing $\tilde{\sigma}_{\nu_e}$ and the e -like fluxes) and without an uncertainty on the NC background in the far detector.

the ν_e and $\bar{\nu}_e$ components) it is possible, in principle, to measure the electron cross sections in the ND. This would lead to a strong reduction of the systematics impact, since then both Φ_{ν_μ} and $\tilde{\sigma}_{\nu_e}$ were known, which is one of the “magic” combinations identified in eq. (2.12). To achieve this situation, in addition to the flux information a careful design of the ND in terms of background rejection and its size is necessary. In this respect we mention that for T2K a liquid Argon detector with a fiducial mass of 0.1 kt is foreseen at 2 km, which would allow to collect a fairly clean sample of ν_e CC events [39].

5.3 Determination of θ_{13} at T2K and T2HK

Let us now discuss the impact of systematics on the θ_{13} measurement. In figure 7 we show the smallest value of $\sin^2 2\theta_{13}$ which can be distinguished from $\theta_{13} = 0$ as a function of the luminosity, assuming two representative values for the CP phase which correspond roughly to the best and worst sensitivity. The first observation is that for T2K phase I systematics have only a small impact, since this measurement is largely dominated by statistics. Numerically we find that the sensitivity of T2K decreases from $\sin^2 2\theta_{13} = 0.0167$ to 0.0172 for $\delta_{CP} = \pi/2$, and from $\sin^2 2\theta_{13} = 0.0206$ to 0.0214 for $\delta_{CP} = \pi$. For T2HK systematics have a non-negligible impact on the θ_{13} discovery reach. The situation is very similar to CPV for small θ_{13} , and the corresponding discussion in section 5.1 largely applies also for the θ_{13} discovery: for this measurement the background dominates in eq. (2.4), and hence the uncertainty on the background is the most relevant systematics. Its impact is controlled by the ability of the ND to predict the background in the FD. We show in figure 7

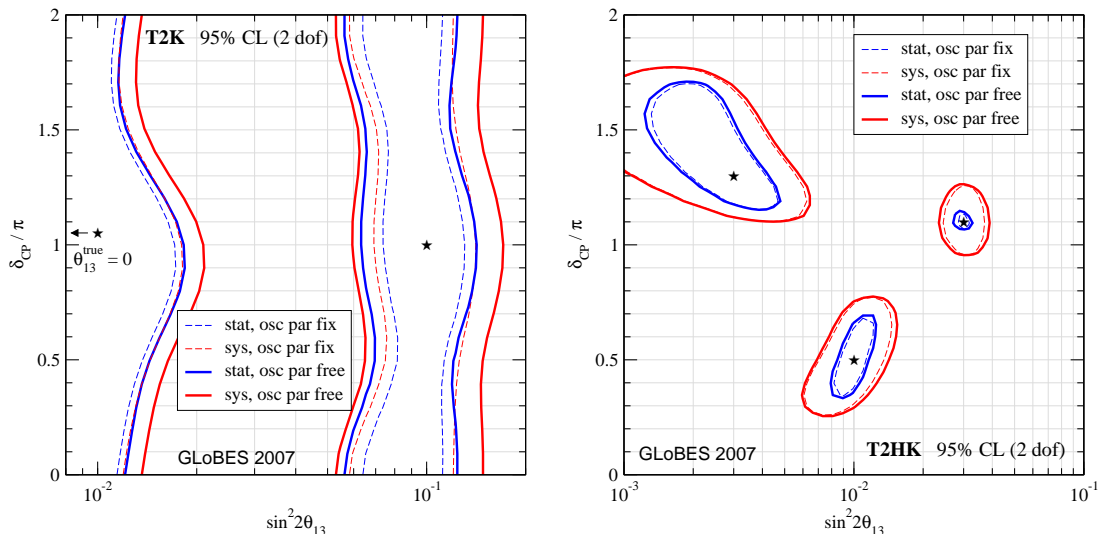


Figure 8: Allowed regions in the plane of $\sin^2 2\theta_{13}$ and δ_{CP} for T2K (left) and T2HK (right) for some example choices for the input values marked by stars in the figures. We show the allowed regions for all combinations of statistical errors only, systematics according to figure 1, all other oscillation parameters fixed, and free (where for the solar parameters we impose present errors). For regions labels “osc par free” we allow also for a 5% uncertainty on the matter density, which however has a negligible impact on the results. The $\text{sign}(\Delta m_{31}^2)$ degeneracy is neglected, and $\theta_{23}^{true} = \pi/4$.

also curves assuming a perfectly known ν_e beam background, and no uncertainty at all on the background (i.e., fixing the ν_e beam contamination as well as the NC background). If the total background is fixed the sensitivity is close to the pure statistics case. It is interesting to note that for the two examples of δ_{CP} shown in the figure the importance of beam and NC backgrounds is different. This is an effect of the spectral shapes of the signal relative to the background, since the spectrum of the signal depends on the value of δ_{CP} , and also beam and NC backgrounds have rather different shapes.

Figure 8 shows the allowed region in the space of $\sin^2 2\theta_{13}$ and δ_{CP} obtained by T2K (left) and T2HK (right) for some example points of “true” parameter values. As expected, for T2K the impact of systematics is small, though not negligible in this case. Furthermore, we show that for T2K the uncertainty on the other oscillation parameters has a sizable impact on the allowed region. We have checked that this effect comes entirely from the atmospheric parameters Δm_{31}^2 and θ_{23} . Apparently the disappearance channel does not provide enough accuracy on these parameters to avoid an effect on the θ_{13} determination. For the solar parameters the accuracy from present data is sufficient to eliminate any effect on the results shown in figure 8.

On the other hand, for T2HK the impact of the correlations with the other oscillation parameters is negligible, since the high statistics sample of the disappearance channel pins down the atmospheric parameters with high precision. In contrast systematics are much more important. For example, for our test point at large θ_{13} ($\sin^2 2\theta_{13} = 0.03$ and $\delta_{CP} = 1.1\pi$) the errors on $\sin^2 2\theta_{13}$ and δ_{CP} are roughly a factor three larger if systematics are included. Clearly in this case the inclusion of systematics would spoil the CPV discovery.

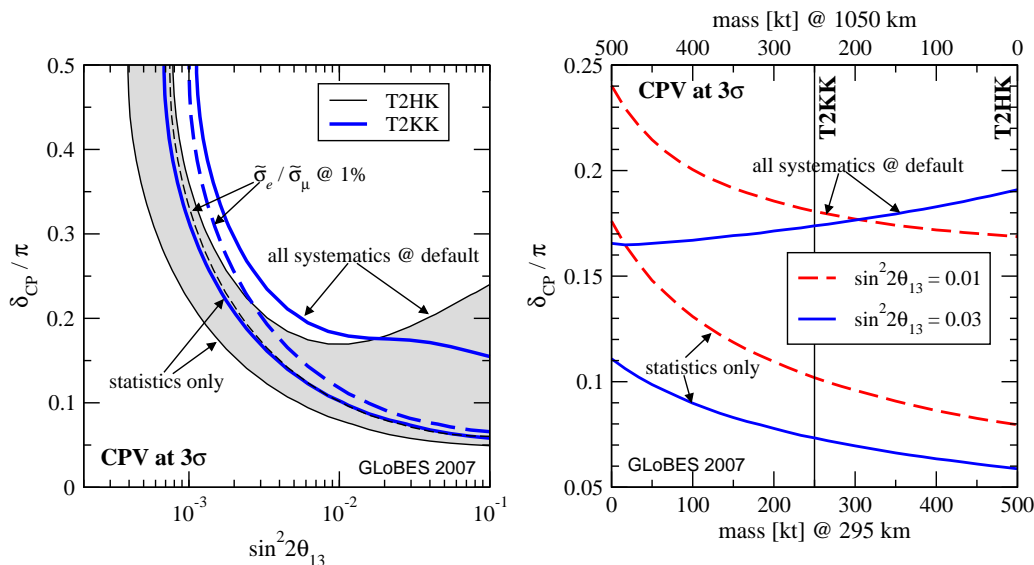


Figure 9: Left hand panel: sensitivity to CPV at 3σ for T2HK and T2KK. Right hand panel: sensitivity to CPV at 3σ for two values of $\sin^2 2\theta_{13}$ by changing the detector mass between Kamioka and Korea.

5.4 T2KK

We have tested also the case when part of the HK detector is moved to Korea, at a baseline of 1050 km. For this analysis we assume that the second FD is located at the same off-axis angle as the first one, like in [17, 54]. For our standard scenario (“T2KK”) we assume a 250 kt detector, both in Kamioka and Korea. The χ^2 construction for the second FD is completely analogous to the ones for the first FD, and we take into account the proper correlations of systematics in the three detector system of ND, FD1, FD2. We focus here on the CPV discovery in order to compare the T2KK and T2HK performances. Needless to say, that a main motivation for having a detector in Korea is to measure the neutrino mass hierarchy which we do not discuss here. The hierarchy determination in turn reduces the impact of degeneracies, which we have not included here in order to focus on the impact of systematics. Such considerations have to be taken into account when evaluating the overall potential of T2KK (which is not the purpose of our discussion).

In the left hand panel of figure 9 the CPV discovery reach of T2KK (blue lines) is shown in comparison to T2HK (shaded region). We find that the pure statistics sensitivity is slightly worse for T2KK. If all systematics are put at our default values splitting the detector yields a somewhat better robustness with respect to systematical uncertainties at large $\sin^2 2\theta_{13} > 10^{-2}$. If precise information on $\tilde{\sigma}_{\nu_e}/\tilde{\sigma}_{\nu_\mu}$ is available T2HK and T2KK perform rather similar. We do not observe a particular cancellation of systematics beyond that already present between near and far detector. Having two baselines makes the physics signal more distinct and unique and hence it is harder for systematical effects to mimic it for large θ_{13} . A similar result was found with a simplified analysis in [55]. Based on these results, it seems not necessary to demand that the two detectors are identical or are located at the same off-axis angle. This is especially important in the context of

the results in [18, 56], which indicate that a more on-axis location for the detector in Korea would greatly enhance the sensitivity to the mass hierarchy. The larger background present at a more on-axis location maybe tolerable, especially if improved algorithms for π^0 identification are used. This issue has been extensively studied in the context of a wide band beam in the US [47–49].

In the right hand panel of figure 9 we show how the discovery reach changes for various distributions of 500 kt fiducial mass between the Korea and Kamioka sites. In the case of statistics only (and neglecting the impact of the hierarchy degeneracy) the conclusion would be that CPV is best discovered by putting all mass to Kamioka. This conclusion changes in presence of systematical errors and now it depends on θ_{13} whether T2KK or T2HK performs better.

6. Summary and discussion

We have studied the impact of a large number of possible systematical errors on the ability of a superbeam experiment to discover CP violation. As a specific example we chose T2HK, however our main results should be applicable to all superbeam experiments using a narrow band beam. We implemented a realistic description of the far detector and included for the first time a near detector in such a study. The emphasis of this work is not to predict the actual sensitivity of a given experiment nor the actual size of systematical errors, but to show that under semi-realistic assumptions the effects are large and need to be studied in more detail. We find that the cancellation of systematics between near and far detectors remains incomplete for the appearance channel, due to a lack of information in the near detector on the final state.

In this respect we have identified two qualitatively different regimes depending on the size of θ_{13} . For small values, close to the sensitivity limit, the main issue is the uncertainty on the background. In this case the performance depends on the ability of the near detector to predict the background in the far detector. In the regime of large θ_{13} ($\sin^2 2\theta_{13} \gtrsim 0.01$, which is probably the more interesting range for this type of experiments) backgrounds are a minor issue and the uncertainty on the signal itself dominates. We find that the impact of systematics even with a near detector is rather strong in this regime. For instance, for T2HK at $\sin^2 2\theta_{13} = 0.1$ the smallest δ_{CP} for which CPV can be established increases from 0.05π for the statistics only case to 0.24π when systematics are included.

However, we were able to identify crucial combinations of parameters, which, when well constrained (at the level of $\lesssim 2\%$) can restore the sensitivity nearly to its statistics only value, namely

- the ratios of the effective ν_μ and ν_e cross sections $\tilde{\sigma}_{\nu_\mu}/\tilde{\sigma}_{\nu_e}$ for neutrinos and anti-neutrinos, or
- the ratios of the effective cross sections between neutrinos and anti-neutrinos, for ν_e and ν_μ , or
- the initial flux of ν_μ and the effective ν_e cross section, both for neutrinos and anti-neutrinos.

With the effective cross section $\tilde{\sigma}$ we mean here the product between physical cross section and detection efficiency. The success of a superbeam experiment in the regime $\sin^2 2\theta_{13} \gtrsim 0.01$ will depend to a significant degree on the information available on these combinations.

Theoretical cross section calculations indicate that the uncertainty on the ratio $\sigma_{\nu_\mu}/\sigma_{\nu_e}$ might actually be at the level of few percent in the T2K energy range of around 700 MeV. However, this result has not been tested experimentally. We stress that this would be a crucial input in the analysis of a superbeam experiment which is not based on any data. Future cross section experiments such as for example MINER ν A may provide a measurement of σ_{ν_μ} at the 5% level. However, from present perspective it seems difficult to obtain a precise measurement for electron neutrino — and especially for electron anti-neutrino cross sections, which are essential for predicting the appearance signal. Maybe the only places where these cross sections can be measured in the relevant energy range are beta beams or a neutrino factory. Note that the absolute normalisation of the cross sections is needed, which always is subject to uncertainties on initial fluxes. Precise information on fluxes may be obtained from Hadron production experiments, such as MIPP, HARP or NA61/SHINE.

Apart from CP violation in T2HK, we find that systematics play a minor role for the θ_{13} discovery sensitivity in T2K (phase I), since this measurement is dominated by statistical errors. For the T2KK setup, where half of the HK detector is moved to Korea, we find that the second far detector helps somewhat in reducing the effect of systematics on the CP violation sensitivity at large θ_{13} . However, this effect does not come from a cancellation of systematics, but from a more robust oscillation signal in the very-far detector. Hence it seems not necessary to demand that the two far detectors are identical or placed at the same off-axis angle.

In order to focus on the impact of systematics we have neglected the hierarchy degeneracy in our study. It is known that for T2HK the presence of the degenerate solution reduces the sensitivity to CPV in a certain range of the parameter space. We have checked that our conclusion on systematics is not changed due to the degeneracy, since also the fake solution is affected in a similar way by systematics as the true one. We stress that for a full evaluation of the CPV sensitivity and a comparison to other experimental options (such as e.g. T2KK) degeneracies have to be included.

Before concluding we add here a few thoughts on whether and how our results may be extrapolated for other facilities, beyond T2HK. Our results indicate that spectral information plays an important role in limiting the effect of systematical uncertainties. This suggests that the behaviour of a wide band superbeam will be different. Without a detailed simulation it is hard to estimate quantitatively whether the impact of systematics is significantly less than in the case of the off-axis configuration considered here, and clearly investigations along these lines would be an interesting topic for future work.

For a beta beam in principle similar considerations apply as in the case of the superbeam, however there are some important differences. First, the initial flux of electron neutrinos is known to good precision. Second, since the signal here is ν_μ appearance, the relevant cross sections are much easier to measure at a MINER ν A type experiment. Hence, it seems easier to constrain the beta beam equivalent of the last combination of quantities listed above, namely ν_e fluxes and ν_μ cross sections. As already mentioned, a close detector

at a beta beam would probably be an ideal place to measure the electron cross sections needed for a superbeam experiment.

The optimal facility concerning systematics seems to be a neutrino factory. In this case intense fluxes of all four flavours $\Phi_{\nu_e}, \Phi_{\bar{\nu}_e}, \Phi_{\nu_\mu}, \Phi_{\bar{\nu}_\mu}$ are available at the near detector, and they are known with very good precision. Hence, all cross sections can be measured accurately at the near detector, which allows to predict the appearance signal in the far detector basically free of systematics on fluxes and cross sections.¹⁰ Nonetheless, it would be useful to actually prove this by explicit calculation.

Acknowledgments

We thank Michele Maltoni for discussions in the initial phase of this work and for providing the routine used for the minimisation of the pull χ^2 , Eligio Lisi for useful comments on a draft of this paper, Davide Meloni for providing the results of [32] in machine readable format, Constantinos Andreopoulos for providing us with GENIE [35] results, Jocelyn Monroe for invaluable clarifications about the MiniBooNE ν_e analysis, Morgan Wascko for useful comments about flux uncertainties, Debbie Harris for a careful reading and a number of suggestions to improve this manuscript, and Natalie Jachowicz for most useful discussions on neutrino cross sections. We acknowledge the support of the European Community-Research Infrastructure Activity under the FP6 ‘‘Structuring the European Research Area’’ program (CARE, contract number RII3-CT-2003-506395).

A. Experiment simulation and systematics treatment

A.1 Detector simulation

The ν_e and $\bar{\nu}_e$ appearance signals in the far detector (FD) are calculated in the following way. We take into account quasi-elastic (QE) as well as non-quasi-elastic (NQE) charged current events using cross sections from the NUANCE v3r503 event generator [34]. However, we require that only a single ring is visible in the detector which strongly reduces the number of NQE events. At the generator level the requirement is that just one particle momentum is above the Čerenkov production threshold. We take into account an energy dependent efficiency for e -like events [16]. Since this efficiency is the product of single ring events plus particle identification for ν_e events, we disentangle the one ring efficiency computed with NUANCE, properly weighted between QE and NQE events, and extract a particle identification efficiency that we assume to be the same for QE, NQE, ν_e and $\bar{\nu}_e$ events. The absolute efficiency is normalised in order to reproduce the total number of signal events provided in table 2 of ref. [16] for given oscillation parameters and 5 yr neutrino data in T2K. We assume the same efficiency function also for anti-neutrino data. For μ -like events we take a flat efficiency of 0.9.

¹⁰We note that in case of the neutrino factory another important systematics (at large θ_{13}) is the uncertainty on the matter density. Its effect on the CP violation sensitivity has been discussed in ref. [57] together with possibilities to reduce it.

The following background sources are included for the ν_e appearance signal (and CP symmetric for the $\bar{\nu}_e$ signal): miss-identified neutral current (NC) events, the intrinsic ν_e and $\bar{\nu}_e$ beam contamination, $\bar{\nu}_e$ events from oscillations of the $\bar{\nu}_\mu$ beam component, and a tiny background from miss-identified muons from ν_μ charged current (CC) events (at a rate of 0.1%). For the NC background we extract the spectral shape and number of events from ref. [16] by scaling to our exposures. Lacking any detailed information for the anti-neutrino mode, we assume the same size and spectrum for the NC background as in the neutrino mode.

For the spectral analysis we take into account the energy reconstruction for QE and NQE events via migration matrices calculated by using NUANCE [34] and SK reconstruction algorithms (see ref. [58], p. 139). We use 50 bins in true neutrino energy from zero to 2 GeV mapped onto 8 bins in reconstructed neutrino energy from 0.4 to 1.2 GeV. In total we apply 8 migration matrices: for QE and NQE events for each neutrino flavour ν_e , $\bar{\nu}_e$, ν_μ , $\bar{\nu}_\mu$. Each matrix is normalised to take into account the single ring efficiency. The migration is consistently applied to signal and ν_e background events. Precise information on our FD simulation including the migration matrices, backgrounds and efficiencies can be recovered from the GLOBES glb-file available at [44].

For the near detector (ND) we assume the idealised situation that the flux is identical to the one of the far detector for no oscillations (i.e., perfect near-to-far extrapolation). For definiteness we take a 0.1 kt detector at a distance of 2 km, for T2K as well as for T2HK. We use the same migration matrices and efficiencies as in the far detector. For the μ -like events we assume no background beyond the events from the ν_μ and $\bar{\nu}_\mu$ beam components. For e -like events we take into account the beam intrinsic ν_e and $\bar{\nu}_e$ fluxes, NC events, as well as miss-identified muons from ν_μ (or $\bar{\nu}_\mu$) CC interactions with a rate of 0.1%. For the NC events we assume the same spectrum as in the FD with the normalisation scaled according to the different mass and baseline of the ND.

A.2 χ^2 definition and systematics

For the statistical analysis we adopt the following χ^2 function based on Poisson statistics in each bin:

$$\chi_{\text{data}}^2(\boldsymbol{\theta}, \xi_\alpha) = 2 \sum_{A=1}^8 \sum_{i=1}^8 \left[T_i^A(\boldsymbol{\theta}, \xi_\alpha) - D_i^A + D_i^A \ln \frac{D_i^A}{T_i^A(\boldsymbol{\theta}, \xi_\alpha)} \right], \quad (\text{A.1})$$

where the index A runs over the 8 data samples in our analysis obtained by all combinations of FD/ND, $\nu/\bar{\nu}$ -beam, and e/μ -like events as given in table 1. The samples 1, 2 (3, 4) correspond to the appearance (disappearance) channels in the FD, whereas samples 5–8 are the ND data. For the T2KK analysis we add 4 more data samples to the ones given in table 1 corresponding to the second FD. In eq. (A.1), $T_i^A(\boldsymbol{\theta}, \xi_\alpha)$ is the theoretical prediction for energy bin i in data sample A , depending on the oscillation parameters $\boldsymbol{\theta}$ and the pulls ξ_α parameterising the systematic uncertainties. Taking only the leading term

A	Detector	Beam	Flavour	A	Detector	Beam	Flavour
1	FD	ν	e -like	5	ND	ν	e -like
2	FD	$\bar{\nu}$	e -like	6	ND	$\bar{\nu}$	e -like
3	FD	ν	μ -like	7	ND	ν	μ -like
4	FD	$\bar{\nu}$	μ -like	8	ND	$\bar{\nu}$	μ -like

Table 1: Data samples.

in the (small) pulls, in general these predictions can be written as¹¹

$$T_i^A(\boldsymbol{\theta}, \xi_\alpha) = N_i^A(\boldsymbol{\theta}) + \sum_\alpha \xi_\alpha \pi_{i\alpha}^A(\boldsymbol{\theta}). \quad (\text{A.2})$$

Note that the T_i^A for the ND ($A = 5, \dots, 8$) do not depend on the oscillation parameters, and hence, the corresponding terms in the χ^2 serve only to constrain the pulls ξ_α . As usual, the corresponding “data” D_i^A is taken as the prediction T_i^A at some assumed “true values” for the oscillation parameters, $\boldsymbol{\theta}^{\text{true}}$, and for zero pulls, i.e., $D_i^A = N_i^A(\boldsymbol{\theta}^{\text{true}})$. The final χ^2 is obtained by adding the penalty terms for the pulls and minimising with respect to them:

$$\chi^2(\boldsymbol{\theta}) = \min_{\xi_\alpha} \left[\chi_{\text{data}}^2(\boldsymbol{\theta}, \xi_\alpha) + \sum_{\alpha=1}^{27} \left(\frac{\xi_\alpha}{\sigma_\alpha} \right)^2 \right]. \quad (\text{A.3})$$

The pull minimisation is performed by using a routine developed by Michele Maltoni.

In our analysis we include 27 independent pulls to account for systematic uncertainties as listed in figure 1 together with the adopted default value for the errors σ_α . They are coupled to the theoretical predictions via the couplings $\pi_{i\alpha}^A$ according to eq. (A.2) accounting for the correct correlations. The pulls 1 and 2 describe the normalisation uncertainties of FD and ND (fiducial mass), correlated between ν - and $\bar{\nu}$ -beams but uncorrelated between the two detectors. Pulls 3–6 take into account the energy calibration uncertainty, correlated between ν - and $\bar{\nu}$ -beams but uncorrelated between the two detectors and e - and μ -like events. Following ref. [39] we adopt a value of 2.5%. The pulls 7–16 account for the flux uncertainties, which are correlated between the two detectors. For each beam we assume all four flavour components to be uncorrelated. For the dominating flux we include in addition a linear tilt on the spectral shape. These errors are representative of the situation without a dedicated hadron production experiment. They are about the same as K2K would have had without the HARP data [6].

Pulls 17–21 parametrise cross section uncertainties. We include an uncorrelated normalisation uncertainty on the total CC cross section for all four neutrino flavours $\nu_e, \nu_\mu, \bar{\nu}_e, \bar{\nu}_\mu$. Note, that pulls 17–21 also account for the effect of the error on the efficiency. Since we assume identical detectors for the FD and ND it seems justified to consider the efficiencies correlated between the detectors, and hence we consider the pulls 17–20 as the effective uncertainty including cross section as well as efficiency uncertainties for the corresponding event types. Pull 21 accounts for the uncertainty on the ratio of QE and NQE

¹¹In our code we use a slightly more complicated pull dependence in order to make sure that the T_i^A stay always positive, which, however, is equivalent to eq. (A.2) at first order in ξ_α .

cross sections, which we take fully correlated between flavours and neutrino/anti-neutrino. K2K has measured this ratio in different near detectors and has found a spread of 20% among the measurements [6], which we adopt as our default value for the uncertainty.

The uncertainty of NC events are taken to be completely uncorrelated between ND and FD. For the FD we include pull 22 for the NC normalisation correlated between ν - and $\bar{\nu}$ -beams, whereas pull 23 accounts for the relative uncertainty. Pulls 24 and 25 account for the NC backgrounds to e -like events in the ND, uncorrelated between ν - and $\bar{\nu}$ -beams. And finally, we include an uncertainty for the rate of muon miss-identification in the ND, again uncorrelated between ν - and $\bar{\nu}$ -beams (pulls 26 and 27). For the T2KK analysis we add 3 more pulls, one for the normalisation and two for the energy calibration of the detector in Korea.

Let us give one explicit example, how the theoretical predictions according to eq. (A.2) are constructed, e.g., for the ν_e appearance channel in the FD ($A = 1$). In this case we have

$$N_i^1 = n_{\nu_\mu \rightarrow \nu_e}^{i,\text{QE}} + n_{\nu_\mu \rightarrow \nu_e}^{i,\text{NQE}} + n_{\text{NC}}^i + n_{\nu_e\text{-beam}}^i + n_{\bar{\nu}_e\text{-beam}}^i + n_{\bar{\nu}_\mu \rightarrow \bar{\nu}_e}^i + n_{\text{miss-ID}}^i. \quad (\text{A.4})$$

The n_x^i correspond to the oscillation signal and the various backgrounds as described above. For simplicity we suppress the dependence on the oscillation parameters, however, in the calculation also oscillations of backgrounds are properly included. Then eq. (A.2) reads

$$\begin{aligned} T_i^1 &= N_i^1(1 + \xi_2) + \xi_5 \pi_{i,\text{calib FD},e}^1 \\ &+ \xi_7 \left(n_{\nu_\mu \rightarrow \nu_e}^{i,\text{QE}} + n_{\nu_\mu \rightarrow \nu_e}^{i,\text{NQE}} + n_{\text{NC}}^i + n_{\text{miss-ID}}^i \right) + \xi_8 \pi_{i,\text{tilt}}^1 \\ &+ \xi_9 n_{\nu_e\text{-beam}}^i + \xi_{10} n_{\bar{\nu}_e\text{-beam}}^i + \xi_{11} n_{\bar{\nu}_\mu \rightarrow \bar{\nu}_e}^i \\ &+ \xi_{17} \left(n_{\nu_\mu \rightarrow \nu_e}^{i,\text{QE}} + n_{\nu_\mu \rightarrow \nu_e}^{i,\text{NQE}} + n_{\nu_e\text{-beam}}^i \right) + \xi_{18} \left(n_{\bar{\nu}_e\text{-beam}}^i + n_{\bar{\nu}_\mu \rightarrow \bar{\nu}_e}^i \right) + \xi_{19} n_{\text{miss-ID}}^i \\ &+ \xi_{21} \left(n_{\nu_\mu \rightarrow \nu_e}^{i,\text{QE}} - n_{\nu_\mu \rightarrow \nu_e}^{i,\text{NQE}} \right) / 2 \\ &+ \xi_{22} n_{\text{NC}}^i + \xi_{23} n_{\text{NC}}^i / 2. \end{aligned} \quad (\text{A.5})$$

Here $\pi_{i,\text{calib FD},e}^1$ and $\pi_{i,\text{tilt}}^1$ account for the energy calibration and ν_μ -flux tilt, respectively. The 6 lines take into account normalisation and calibration, ν_μ -flux uncertainty, uncertainties of the other flux components, total cross section and efficiency uncertainties, the QE/NQE ratio, and NC uncertainties. The last line for the $\bar{\nu}$ -beam ($A = 2$) would read $+\xi_{22} n_{\text{NC}}^i - \xi_{23} n_{\text{NC}}^i / 2$ in order to account for the correlations of the NC pulls as described above. The T_i^A for the other samples are defined in an analogous way. Through this construction we make sure that we use only the information which is actually provided by the ND measurements.

B. A far detector-only setup with effective systematics

Previous sensitivity studies (such as for example the ones in refs. [15, 40, 37]) do not include a ND in the simulation, and some values for systematical uncertainties are adopted, which are assumed to implicitly encode information from the ND. In this appendix we examine in which way such choices for systematical errors should be interpreted. We calculate

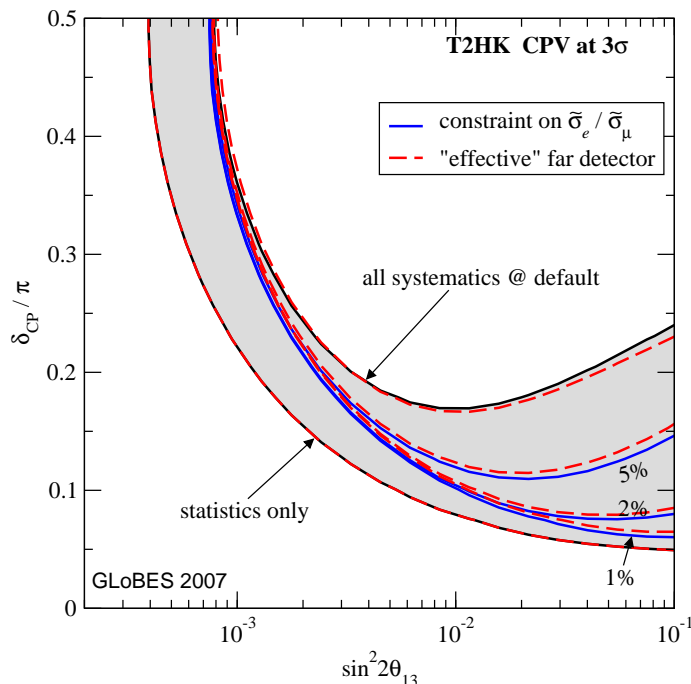


Figure 10: Comparison of the effective FD description (dashed curves) with the full ND/FD setup. The shaded region, as well as the blue curves correspond to our standard simulation and are identical to the corresponding curves in figure 2.

the sensitivity to CPV for T2HK for a FD-only configuration (denoted by FD^{eff}), by using exactly the same detector simulation and backgrounds as before, but we include only four independent effective systematical uncertainties: the normalisations of the appearance signal and the normalisations of the total background, both for neutrinos and anti-neutrinos ($\sigma_{\nu}^{\text{sig}}, \sigma_{\bar{\nu}}^{\text{sig}}, \sigma_{\nu}^{\text{bg}}, \sigma_{\bar{\nu}}^{\text{bg}}$). According to the discussion in section 2 one expects that σ_{ν}^{bg} and $\sigma_{\bar{\nu}}^{\text{bg}}$ will be relevant for the sensitivity at small θ_{13} , whereas $\sigma_{\nu}^{\text{sig}}$ and $\sigma_{\bar{\nu}}^{\text{sig}}$ will dominate the sensitivity at large θ_{13} , and this is indeed the behaviour we find.

In figure 10 we compare this FD^{eff} simulation with the full ND/FD configuration. As it must be, the pure statistics sensitivities are identical. It turns out that the ND/FD sensitivity with all systematics at the default values according to figure 1 is reproduced rather accurately by FD^{eff} for the following choice of systematics:

$$\sigma_{\nu}^{\text{sig}} = \sigma_{\bar{\nu}}^{\text{sig}} = 10\%, \quad \sigma_{\nu}^{\text{bg}} = \sigma_{\bar{\nu}}^{\text{bg}} = 3.5\%. \quad (\text{B.1})$$

We conclude from these numbers that our specific implementation of the ND provides a 3.5% measurement of the background, whereas the effective error on the signal turns out to be 10%. To reproduce the curves corresponding to a constraint on the $\tilde{\sigma}_{\nu_e}/\tilde{\sigma}_{\nu_\nu}$ ratio at $x\%$ in the full ND/FD case, one simply has to set $\sigma_{\nu}^{\text{sig}} = \sigma_{\bar{\nu}}^{\text{sig}} = x\%$ for FD^{eff} . This confirms the arguments given in section 2, that the error on the ratio $\tilde{\sigma}_{\nu_e}/\tilde{\sigma}_{\nu_\nu}$ directly translates into an error on the appearance signal.

The FD^{eff} calculations can be performed with a standard GLOBES analysis. A glb-file for this effective FD simulation for T2HK is available at [44].

References

- [1] SUPER-KAMKIOKANDE collaboration, J. Hosaka et al., *Solar neutrino measurements in Super-Kamiokande-I*, *Phys. Rev. D* **73** (2006) 112001 [[hep-ex/0508053](#)].
- [2] SNO collaboration, B. Aharmim et al., *Electron energy spectra, fluxes, and day-night asymmetries of B-8 solar neutrinos from the 391-day salt phase SNO data set*, *Phys. Rev. C* **72** (2005) 055502 [[nucl-ex/0502021](#)].
- [3] SUPER-KAMKIOKANDE collaboration, Y. Ashie et al., *A measurement of atmospheric neutrino oscillation parameters by Super-Kamiokande I*, *Phys. Rev. D* **71** (2005) 112005 [[hep-ex/0501064](#)].
- [4] A. Kozlov, *KamLAND current status & future prospects*, talk given at *Workshop on Next generation Nucleon decay and Neutrino detectors*, NNN, http://www-rcn.icrr.u-tokyo.ac.jp/NNN07/Oct3/06-Kozlov_NNN07.pdf, Hamamatsu Japan (2007).
- [5] KAMLAND collaboration, T. Araki et al., *Measurement of neutrino oscillation with KamLAND: evidence of spectral distortion*, *Phys. Rev. Lett.* **94** (2005) 081801 [[hep-ex/0406035](#)].
- [6] K2K collaboration, M.H. Ahn et al., *Measurement of neutrino oscillation by the K2K experiment*, *Phys. Rev. D* **74** (2006) 072003 [[hep-ex/0606032](#)].
- [7] K2K collaboration, E. Aliu et al., *Evidence for muon neutrino oscillation in an accelerator-based experiment*, *Phys. Rev. Lett.* **94** (2005) 081802 [[hep-ex/0411038](#)].
- [8] MINOS collaboration, D.G. Michael et al., *Observation of muon neutrino disappearance with the MINOS detectors and the NuMI neutrino beam*, *Phys. Rev. Lett.* **97** (2006) 191801 [[hep-ex/0607088](#)].
- [9] LSND collaboration, A. Aguilar et al., *Evidence for neutrino oscillations from the observation of $\bar{\nu}/e$ appearance in a $\bar{\nu}/\mu$ beam*, *Phys. Rev. D* **64** (2001) 112007 [[hep-ex/0104049](#)].
- [10] F. Dydak et al., *A search for muon-neutrino oscillations in the Δm^2 range 0.3 eV^2 to 90 eV^2* , *Phys. Lett. B* **134** (1984) 281.
- [11] Y. Declais et al., *Search for neutrino oscillations at 15-meters, 40-meters, and 95-meters from a nuclear power reactor at Bugey*, *Nucl. Phys. B* **434** (1995) 503.
- [12] MINIBOONE collaboration, A.A. Aguilar-Arevalo et al., *A search for electron neutrino appearance at the $\Delta m^2 \sim 1 \text{ eV}^2$ scale*, *Phys. Rev. Lett.* **98** (2007) 231801 [[arXiv:0704.1500](#)].
- [13] M. Maltoni and T. Schwetz, *Sterile neutrino oscillations after first MiniBooNE results*, *Phys. Rev. D* **76** (2007) 093005 [[arXiv:0705.0107](#)].
- [14] P. Huber, M. Lindner, M. Rolinec, T. Schwetz and W. Winter, *Prospects of accelerator and reactor neutrino oscillation experiments for the coming ten years*, *Phys. Rev. D* **70** (2004) 073014 [[hep-ph/0403068](#)].
- [15] THE ISS PHYSICS WORKING GROUP collaboration, *Physics at a future neutrino factory and super-beam facility*, [arXiv:0710.4947](#).
- [16] T2K collaboration, Y. Itow et al., *The JHF-Kamioka neutrino project*, [hep-ex/0106019](#).

- [17] M. Ishitsuka, T. Kajita, H. Minakata and H. Nunokawa, *Resolving neutrino mass hierarchy and CP degeneracy by two identical detectors with different baselines*, *Phys. Rev. D* **72** (2005) 033003 [[hep-ph/0504026](#)].
- [18] K. Hagiwara, N. Okamura and K.-i. Senda, *Solving the neutrino parameter degeneracy by measuring the T2K off-axis beam in Korea*, *Phys. Lett. B* **637** (2006) 266 [*Erratum ibid.* **B 641** (2006) 486] [[hep-ph/0504061](#)].
- [19] P. Huber, M. Lindner, T. Schwetz and W. Winter, *Reactor neutrino experiments compared to superbeams*, *Nucl. Phys. B* **665** (2003) 487 [[hep-ph/0303232](#)].
- [20] DOUBLE CHOOZ collaboration, F. Ardellier et al., *Double chooz, a search for the neutrino mixing angle θ_{13}* , [hep-ex/0606025](#).
- [21] PARTICLE DATA GROUP collaboration, W.M. Yao et al., *Review of particle physics*, *J. Phys. G* **33** (2006) 1.
- [22] C.H. Llewellyn Smith, *Neutrino reactions at accelerator energies*, *Phys. Rept.* **3** (1972) 261.
- [23] A. Bodek, S. Avvakumov, R. Bradford and H. Budd, *Extraction of the axial nucleon form factor from neutrino experiments on deuterium*, [arXiv:0709.3538](#).
- [24] R.A. Smith and E.J. Moniz, *Neutrino reactions on nuclear targets*, *Nucl. Phys. B* **43** (1972) 605 [*Erratum ibid.* **B 101** (1975) 547].
- [25] V. Bernard, L. Elouadrhiri and U.G. Meissner, *Axial structure of the nucleon*, *J. Phys. G* **28** (2002) R1 [[hep-ph/0107088](#)].
- [26] K2K collaboration, R. Gran et al., *Measurement of the quasi-elastic axial vector mass in neutrino oxygen interactions*, *Phys. Rev. D* **74** (2006) 052002 [[hep-ex/0603034](#)].
- [27] MINIBOONE collaboration, A.A. Aguilar-Arevalo et al., *Measurement of muon neutrino quasi-elastic scattering on carbon*, *Phys. Rev. Lett.* **100** (2008) 032301 [[arXiv:0706.0926](#)].
- [28] S.K. Singh and E. Oset, *Quasielastic neutrino (anti-neutrino) reactions in nuclei and the axial vector form-factor of the nucleon*, *Nucl. Phys. A* **542** (1992) 587.
- [29] MINIBOONE collaboration, J. Monroe, *Charged current quasi-elastic interactions at MiniBooNE confront cross section Monte Carlos*, *Nucl. Phys.* **139** (*Proc. Suppl.*) (2005) 59 [[hep-ex/0408019](#)].
- [30] E. Kolbe, K. Langanke, G. Martinez-Pinedo and P. Vogel, *Neutrino nucleus reactions and nuclear structure*, *J. Phys. G* **29** (2003) 2569 [[nucl-th/0311022](#)].
- [31] M. Valverde, J.E. Amaro and J. Nieves, *Theoretical uncertainties on quasielastic charged-current neutrino nucleus cross sections*, *Phys. Lett. B* **638** (2006) 325 [[hep-ph/0604042](#)].
- [32] O. Benhar and D. Meloni, *Total neutrino and antineutrino nuclear cross sections around 1 GeV*, *Nucl. Phys. A* **789** (2007) 379 [[hep-ph/0610403](#)].
- [33] J. Nieves, J.E. Amaro and M. Valverde, *Inclusive quasielastic charged-current neutrino-nucleus reactions*, *Phys. Rev. C* **70** (2004) 055503 [*Erratum ibid.* **C 72** (2005) 019902] [[nucl-th/0408005](#)].
- [34] D. Casper, *The nuance neutrino physics simulation, and the future*, *Nucl. Phys.* **112** (*Proc. Suppl.*) (2002) 161 [[hep-ph/0208030](#)].

- [35] C. Andreopoulos, *The GENIE universal, object-oriented neutrino generator*, *Nucl. Phys.* **159** (Proc. Suppl.) (2006) 217.
- [36] H. Gallagher, *The NEUGEN neutrino event generator*, *Nucl. Phys.* **112** (Proc. Suppl.) (2002) 188.
- [37] J.E. Campagne, M. Maltoni, M. Mezzetto and T. Schwetz, *Physics potential of the CERN-MEMPHYS neutrino oscillation project*, *JHEP* **04** (2007) 003 [[hep-ph/0603172](#)].
- [38] J.R. Monroe, *A combined ν/μ and ν/e oscillation search at MiniBooNE*, FERMILAB-THESIS-2006-44.
- [39] T2K collaboration, *A letter of intent to extend T2K with a detector 2 km away from the JPARC neutrino source*, (2007).
- [40] P. Huber, M. Lindner and W. Winter, *Superbeams versus neutrino factories*, *Nucl. Phys.* **B 645** (2002) 3 [[hep-ph/0204352](#)].
- [41] G.L. Fogli, E. Lisi, A. Marrone, D. Montanino and A. Palazzo, *Getting the most from the statistical analysis of solar neutrino oscillations*, *Phys. Rev.* **D 66** (2002) 053010 [[hep-ph/0206162](#)].
- [42] P. Huber, M. Lindner and W. Winter, *Simulation of long-baseline neutrino oscillation experiments with GLoBES*, *Comput. Phys. Commun.* **167** (2005) 195 [[hep-ph/0407333](#)].
- [43] P. Huber, J. Kopp, M. Lindner, M. Rolinec and W. Winter, *New features in the simulation of neutrino oscillation experiments with GLoBES 3.0*, *Comput. Phys. Commun.* **177** (2007) 432 [[hep-ph/0701187](#)].
- [44] *GLoBES General Long Baseline Experiment Simulator*, <http://www.mpi-hd.mpg.de/lin/globes/>.
- [45] MINERVA collaboration, D. Drakoulakos et al., *Proposal to perform a high-statistics neutrino scattering experiment using a fine-grained detector in the NuMI beam*, [hep-ex/0405002](#).
- [46] SciBooNE collaboration, A.A. Aguilar-Arevalo et al., *Bringing the SciBar detector to the booster neutrino beam*, [hep-ex/0601022](#).
- [47] V. Barger et al., *Precision physics with a wide band super neutrino beam*, *Phys. Rev.* **D 74** (2006) 073004 [[hep-ph/0607177](#)].
- [48] M. Diwan et al., *Proposal for an experimental program in neutrino physics and proton decay in the homestake laboratory*, [hep-ex/0608023](#).
- [49] V. Barger et al., *Report of the U.S. long baseline neutrino experiment study*, [arXiv:0705.4396](#).
- [50] R. Raja, *The Main Injector Particle Production experiment (MIPP) at Fermilab*, *Nucl. Instrum. Meth.* **A553** (2005) 225 [[hep-ex/0501005](#)].
- [51] HARP collaboration, M.G. Catanesi et al., *The HARP detector at the Cern PS*, *Nucl. Instrum. Meth.* **A571** (2007) 527.
- [52] M.G. Catanesi et al., *Measurement of the production cross-section of positive pions in the collision of 8.9 GeV/c protons on beryllium*, *Eur. Phys. J.* **C 52** (2007) 29 [[hep-ex/0702024](#)].
- [53] NA61 collaboration, A. Laszlo et al., *NA61/Shine at the CERN SPS*, [arXiv:0709.1867](#).

- [54] T. Kajita, H. Minakata, S. Nakayama and H. Nunokawa, *Resolving eight-fold neutrino parameter degeneracy by two identical detectors with different baselines*, *Phys. Rev. D* **75** (2007) 013006 [[hep-ph/0609286](#)].
- [55] V. Barger, P. Huber, D. Marfatia and W. Winter, *Which long-baseline neutrino experiments are preferable?*, *Phys. Rev. D* **76** (2007) 053005 [[hep-ph/0703029](#)].
- [56] K. Hagiwara, N. Okamura and K.-i. Senda, *Physics potential of T2KK: an extension of the T2K neutrino oscillation experiment with a far detector in Korea*, *Phys. Rev. D* **76** (2007) 093002 [[hep-ph/0607255](#)].
- [57] P. Huber, M. Lindner, M. Rolinec and W. Winter, *Optimization of a neutrino factory oscillation experiment*, *Phys. Rev. D* **74** (2006) 073003 [[hep-ph/0606119](#)].
- [58] H. Maesaka, *Evidence for muon neutrino oscillation in an accelerator-based experiment*, Ph.D. thesis, Kyoto University, Japan (2005).